Shadowing and Antishadowing of Nuclear Structure Functions

Stanley J. Brodsky and Hung Jung Lu

Stanford Linear Accelerator Center, Stanford University, Stanford, California 94309

(Received 25 September 1989)

The observed shadowing and antishadowing phenomena of quark structure functions in nuclei at small x are interpreted as a consequence of an antiquark-nucleus multiscattering process.

One of the most striking nuclear effects seen in the deep-inelastic structure functions is the depletion of the effective number of nucleons F_2^A/F_2^N in the region of low x. The results from the European Muon Collaboration[1] (EMC) indicate that the effect is roughly Q^2 independent; i.e., shadowing is a leading twist in the operator-product analysis. In contrast, the shadowing of the real photoabsorption cross section due to ρ dominance[2-5] falls away as an inverse power of Q^2.

Shadowing is a destructive interference effect which causes a diminished flux and interactions in the interior and back face of the nucleus. The Glauber analysis[6] of hadron-nucleus scattering corresponds to the following: The incident hadron scatters elastically on a nucleon N_1 on the front face of the nucleus. At high energies the phase of the amplitude is imaginary. The hadron then propagates through the nucleus to nucleon N_2, where it interacts inelastically. The accumulated phase of the hadron propagator is also imaginary, so that this two-step amplitude is coherent and opposite in phase to the one-step amplitude where the beam hadron interacts directly on N_2 without initial-state interactions. Thus the target nucleon N_2 sees less incoming flux: It is shadowed by elastic interactions on the front face of the nucleus. If the hadron-nucleon cross section is large, then for large A the effective number of nucleons participating in the inelastic interactions is reduced to $\sim A^{2/3}$, the number of surface nucleons.

In the case of virtual photoabsorption, the photon converts to a $q\bar{q}$ pair at a distance before the target proportional to $\omega = x^{-1} = 2p \cdot q/Q^2$ in the laboratory frame.[7] In a physical gauge, such as the light-cone $A^+ = 0$ gauge, the final-state interactions of the quark can be neglected in the Bjorken limit, and effectively only the antiquark interacts. The nuclear structure function F_2^A producing quark q can then be written as an integral[8,9] over the inelastic cross section $\sigma_{\bar{q}A}(s')$, where s' grows as $1/x$ for fixed spacelike antiquark mass. Thus the A dependence of the cross section mimics the A dependence of the $\bar{q}$ cross section in the nucleus. We have applied the standard Glauber multiscattering theory to $\sigma_{\bar{q}A}$ assuming that formalism can be taken over to off-shell $\bar{q}$ interactions (the shadowing mechanism is illustrated in Fig. 1). Our results show that for reasonable values of the $\bar{q}$-nucleon cross section, one can understand the mag-

nitude of the shadowing effect at small x. Moreover, if one introduces an $\alpha_R \simeq \frac{1}{2}$ Reggeon contribution to the $\bar{q}N$ amplitude, the real phase introduced by such a contribution automatically leads to "antishadowing" [effective number of nucleons $F_2^A(x,Q^2)/F_2^N(x,Q^2) > A$] at $x \simeq 0.15$ of the few-percent magnitude seen by the SLAC and EMC experiments.[1,10]

Our analysis provides the input or starting point for the $\log Q^2$ evolution of the deep-inelastic structure functions, as given, for example, by Mueller and Qiu.[11] The parameters for the effective $\bar{q}$-nucleon cross section required to understand shadowing phenomena provide important information on the interactions of quarks in nuclear matter. Our analysis also has implications of the nature of particle production for virtual photoabsorption in nuclei. At high Q^2 and $x > 0.3$, hadron production should be uniform throughout the nucleus. At low x or at low Q^2, where shadowing occurs, the inelastic reaction occurs mainly at the front surface. These features can
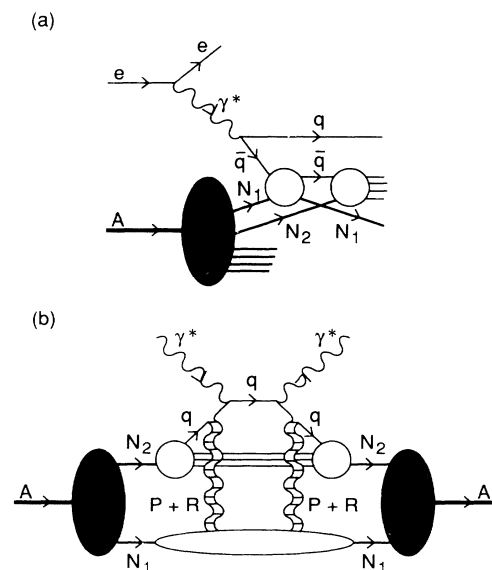
(a)

(b)

FIG. 1. (a) The double-scattering amplitude that shadows the direct interaction of the antiquark with N_2. (b) The same mechanism as in (a), drawn in the traditional "hand-bag" form. The Pomeron and Reggeon exchanges between the quark line and N_1 are explicitly illustrated.

be examined in detail by studying nonadditive multiparticle correlations in both the target and current fragmentation region.

Recently, Frankfurt and Strikman proposed a model for the shadowing and antishadowing of the leading-twist nuclear structure function in the small-x region.[12] Their approach differs with ours in two ways: (1) They apply Glauber's formula in the spirit of a vector-meson-dominance calculation in an aligned jet model, hence their analysis essentially aims toward the lower-Q^2 region ($Q^2 \leq 4$ GeV^2). (2) The antishadowing effect is required on the basis of a sum rule rather than attributed to any particular dynamical mechanism.

We shall neglect the quark spin degrees of freedom in our analysis. The distribution functions of spinless partons in the nucleon and nucleus are, respectively,[8,9]

$$xf^N(x) = \frac{2}{(2\pi)^3} \frac{Cx^2}{1-x} \int ds\, d^2k_\perp \text{Im}T_R^N(s,\mu^2), \quad (1)$$

and

$$xf^A(x) = \frac{2}{(2\pi)^3} \frac{Cx^2}{1-x} \int ds\, d^2k_\perp \text{Im}T_R^A(s,\mu^2), \quad (2)$$

where the integral is over the right-hand cut of the forward $\bar{q}$-nucleon [or $\bar{q}$-nucleus] scattering amplitude $\text{Im}T_R^N(s,\mu^2)$ [$\text{Im}T_R^A(s,\mu^2)$], which includes the propagators of the partons. We will assume the amplitudes vanish as $\mu^2 \to -\infty$, where

$$\mu^2 = -x(s+k_\perp^2)/(1-x) + xM^2 - k_\perp^2 \quad (3)$$

is the invariant four-momentum squared of the interacting parton. The constant C incorporates the parton wave-function renormalization constant,[9] M is the mass of nucleon, and $k_\perp$ is the parton's transverse momentum.

The scaled effective number of nucleons for fixed x is defined as ($v^2 = -\mu^2$)

$$\frac{A_{\text{eff}}(x)}{A} = \frac{F_2^A(x)}{AF_2^N(x)} = \frac{xf^A(x)}{Axf^N(x)}$$

$$= \frac{\int ds\, d^2k_\perp \text{Im}T_R^A(s,v^2)}{A\int ds\, d^2k_\perp \text{Im}T_R^N(s,v^2)}. \quad (4)$$

We have implicitly considered an "average parton," that is, $f^A(x)$ and $f^N(x)$ are the distribution functions averaged over all the quark and antiquark flavors.

In general, we expect the $\bar{q}$-A scattering amplitude can be obtained from the $\bar{q}$-N amplitude via Glauber's theory.[13] We assume that the high-energy antiquark-nucleon scattering amplitude $T_{\bar{q}N}$ has the Regge and analytic behavior characteristic of normal hadronic amplitudes even though quarks do not appear as asymptotic states. This can be justified on the basis of the factorization of Regge singularities, and the fact that at low x the $\bar{q}$ propagates over a distance proportional to $1/x$ in the target rest frame.[14] For our model we include a standard Reggeon at $\alpha_R = \frac{1}{2}$ and a term at $\alpha_R = -1$, in addition to the Pomeron-exchange term [the diagram corresponding to these contributions is shown in Fig. 1(b)]:

$$T_{\bar{q}N}(s,v^2) = \sigma[is\beta_1(v^2) + (1-i)s^{1/2}\beta_{1/2}(v^2)$$
$$+ is^{-1}\beta_{-1}(v^2)]. \quad (5)$$

(Note this is the amputated $\bar{q}$-N amplitude, i.e., by attaching the external parton propagators to $T_{\bar{q}N}$ we recover the nonamputated amplitude T_R^N.) For large s, the Pomeron term dominates and $T_{\bar{q}N}$ becomes imaginary, thus leading to the shadowing effect for small x. However, at lower values of s the real part is important, and we shall see this leads to an antishadowing enhancement of the $\bar{q}$-A amplitude. The main role of the $\alpha_R = -1$ term in the parametrization (5) is to simulate the valence-quark contribution in the low-x domain. Further terms can be added, but these three terms reflect the essential properties of parton distribution functions needed here to study the low-x region (see Fig. 2). The phase of the $\alpha_R = -1$ term is imaginary in the forward Compton amplitude, corresponding by the optical theorem to a conventional "photoelectric effect" in the production cross section.

We assume a Gaussian wave function for the nucleons in the nucleus,[15-17]

$$|\Psi(r_1,\ldots,r_A)|^2 = \prod_{j=1}^A (\pi R^2)^{3/2}\exp(-r_j^2/R^2),$$
$$\quad (6)$$
$$R^2 = \tfrac{2}{3}R_0^2, \quad R_0 = 1.123A^{1/3} \text{ fm},$$

and adopt the usual parametrization for the high-energy particle-nucleon scattering amplitude,

$$T_{\bar{q}N}(s,v^2,\mathbf{q}) = T_{\bar{q}N}(s,v^2)\exp(-\tfrac{1}{2}b\mathbf{q}^2), \quad (7)$$
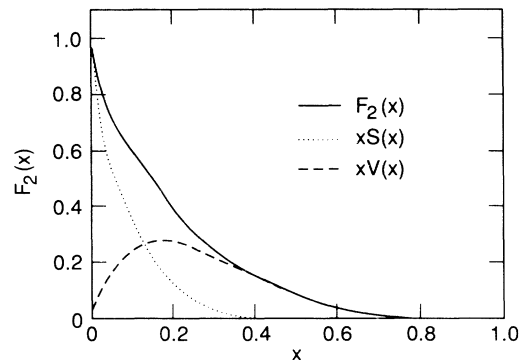

FIG. 2. The computed nucleon structure function $F_2(x)$ assuming the set of parameters in Table I and normalized such that $F_2(0) = 1$. In order to show separate sea distribution $xS(x)$ and valence distribution $xV(x)$, we have assumed the following parametrization:

$$T_{\bar{q}N}^{\text{sea}}(s,v^2) = \sigma[is\beta_1(v^2) + 1.2(1-i)s^{1/2}\beta_{1/2}(v^2)],$$

$$T_{\bar{q}N}^{\text{valence}}(s,v^2) = \sigma[-0.2(1-i)s^{1/2}\beta_{1/2}(v^2) + is^{-1}\beta_{-1}(v^2)].$$

where $\mathbf{q}^2 \simeq -q^2$ is the square of the transferred momentum in the laboratory frame.

Glauber's analysis[15-17] yields[18]

$$T_{\bar{q}A}(s,v^2) = T_{\bar{q}N}(s,v^2)$$

$$\times \sum_{j=1}^{A} \frac{1}{j} \begin{pmatrix} A \\ j \end{pmatrix} \left(\frac{iT_{\bar{q}N}(s,v^2)}{4\pi p_{\mathrm{c.m.}} s^{1/2}(R^2+2b)} \right)^{j-1} .$$

$$(8)$$

After attaching the propagators to the amplitudes in (5) and (8), the ratio

$$\frac{A_{\mathrm{eff}}(x)}{A} = \frac{\int ds\, d^2k_\perp \, \mathrm{Im}\, T_{\bar{q}A}(s,v^2)\Delta_F^2(v^2)}{A \int ds\, d^2k_\perp \, \mathrm{Im}\, T_{\bar{q}N}(s,v^2)\Delta_F^2(v^2)} \qquad (9)$$

can be evaluated numerically.

We shall assume that $T_{\bar{q}N}(s,v^2)$ vanishes as an inverse power of v^2 at large spacelike quark mass. We take

$$\beta_a(v^2) = \frac{f_a}{1+(v^2/\bar{v}_a^2)^{n_a}}, \qquad (10)$$

where $a = 1, \frac{1}{2}, -1$. The characteristic scale for the Pomeron and the $a_R = \frac{1}{2}$ Reggeon is taken to be $\bar{v}_1^2, \bar{v}_{1/2}^2 \simeq 0.30$ GeV^2. The $a_R = -1$ valence term is assumed to fall off at the nucleon mass scale: $\bar{v}_{-1}^2 \simeq 1$ GeV^2. In order to give a short momentum range behavior to the Pomeron and the $a_T = \frac{1}{2}$ Reggeon we fix $n_1 = 4$, and we assign $n_{-1} = 2$ to provide the long tail necessary for larger-x behavior of the valence-quark distribution function. By definition $f_1 = 1$, whereas $f_{1/2}$ and f_{-1} are adjusted consistently with the shape of the nucleon structure function at low x. The propagator of the antiquark lines in the nonamputated amplitudes is assumed to have a monopole form on the spacelike quark mass:

$$i\Delta_F(v^2) \propto \frac{1}{\bar{v}_p^2 + v^2}. \qquad (11)$$

A summary of the set of parameters used is given in Table I. The resulting nucleon structure function computed from Eq. (1) is shown in Fig. 2. The valence-quark contributions are associated with both the $a = \frac{1}{2}$ and $a = -1$ terms. Figure 2 shows that the parametrization used in our analysis for $T_{\bar{q}N}$ gives a reasonable accounting of the various components to the structure function of F_2^N at low x in accord with conventional phenomenology.

TABLE I. Value of parameters used in the multiscattering model.

σ	30 mb	$f_{1/2}$	0.90 GeV
$\bar{v}_1^2, \bar{v}_{1/2}^2, \bar{v}_p^2$	0.30 GeV^2	f_{-1}	0.20 GeV^4
$\bar{v}_{-1}^2$	1.00 GeV^2	M^2	0.88 GeV^2
$n_1, n_{1/2}$	4	s^*	1.52 GeV^2
n_{-1}	2	b	10 (GeV/c)$^{-2}$

We can now compute the nuclear structure function and the ratio $A_{\mathrm{eff}}(x)/A$ from Eq. (9). The results are given in Fig. 3 for $A = 12$, 64, and 238. One observes shadowing below $x \simeq 0.1$ and an antishadowing peak around $x \simeq 0.15$. The shadowing effects are roughly logarithmic on the mass number A. The magnitude of shadowing predicted by the model is consistent with the data for $x > 0.01$; below this region, one expects higher-twist and vector-meson-dominance shadowing to contribute. For $x > 0.2$ other nuclear effects must be taken into account. Most of the parameters used in the model are assigned typical hadronic values, but σ and $f_{1/2}$ deserve more explanation. Here, σ controls the magnitude of the shadowing effect near $x = 0$: A large value of σ implies a larger $\bar{q}^*N$ cross section and thus more shadowing. Notice that σ is the effective cross section at zero $\bar{q}$ virtuality, thus the typical value $\langle\sigma\rangle$ entering the calculation is somewhat smaller. A variation in the parameter $f_{1/2}$ modifies the amount of antishadowing by altering the real-to-imaginary-part ratio of the scattering amplitude.

Our semiquantitative analysis shows that parton multiple-scattering process provides a mechanism for explaining the observed shadowing at low x in the EMC-SLAC data. The existence of antishadowing requires the presence of regions where the real part of the $\bar{q}$-N amplitude dominates over the imaginary part. The constructive interference which gives antishadowing in the $x \sim 0.15$ region is due in this model to the phase of the Reggeon $a = \frac{1}{2}$ term. The phase follows from analyticity and is dictated by the shape of the structure functions at low x. We could utilize additional terms (at lower values of a) to parametrize other bound-state contributions which vanish as higher powers of x, but in practice their qualitative effect would be indistinguishable from our simplified model.

The analysis presented here correlates shadowing phenomena to microscopic quark-nucleon parameters. This approach also provides a dynamical and analytic ex-
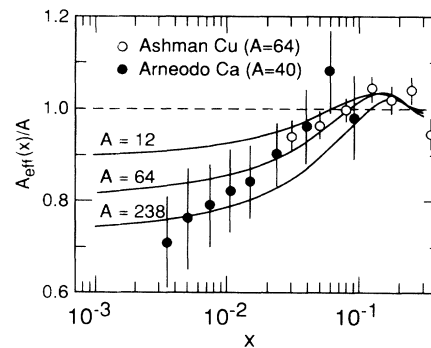

FIG. 3. The predicted ratio of $A_{\mathrm{eff}}(x)/A$ of the multiscattering model in the low-x region for different nuclear mass number. The data points are results from the EMC experiment for Cu and Ca.

planation of antishadowing; previous treatments simply argued for the existence of such a contribution on the basis of conservation laws, but with no predictive power on where in x it should occur, its magnitude, etc. Using the perturbative QCD factorization theorem for inclusive reactions, the same analysis can be extended to Drell-Yan and other fusion processes, taking into account the separate dependence on the valence and sea quarks. Thus some shadowing and antishadowing should also be observable in the nuclear structure function $F_2^A(x_2, Q^2)$ extracted from massive lepton-pair production on nuclear targets at low x_2.

[1]J. Ashman et al., Phys. Lett. B **202**, 603 (1988); CERN Report No. CERN-EP/88-06, 1988 (unpublished); M. Arneodo et al., Phys. Lett. B **211**, 493 (1988).

[2]J. S. Bell, Phys. Rev. Lett. **13**, 57 (1964).

[3]L. Stodolsky, Phys. Rev. Lett. **18**, 135 (1967).

[4]S. J. Brodsky and J. Pumplin, Phys. Rev. **182**, 1794 (1969).

[5]J. J. Sakurai and D. Schildknecht, Phys. Lett. **40B**, 121 (1972); **41B**, 489 (1972); **42B**, 216 (1972).

[6]R. J. Glauber, in Lectures in Theoretical Physics, edited by W. E. Brittin et al. (Interscience, New York, 1959), Vol. I.

[7]T. H. Bauer, R. D. Spital, D. R. Yennie, and F. M. Pipkin, Rev. Mod. Phys. **50**, 261 (1978).

[8]P. V. Landshoff, J. C. Polkinghorne, and R. D. Short, Nucl. Phys. **B28**, 225 (1971).

[9]S. J. Brodsky, F. E. Close, and J. F. Gunion, Phys. Rev. D **5**, 1384 (1972).

[10]R. G. Arnold et al., Phys. Rev. Lett. **52**, 727 (1984); SLAC Report No. SLAC-PUB-3257, 1983 (unpublished).

[11]A. H. Mueller and J. Qiu, Nucl. Phys. **B268**, 427 (1986); J. Qiu, Nucl. Phys. **B291**, 746 (1987).

[12]L. L. Frankfurt and M. I. Strikman, Nucl. Phys. **B316**, 340 (1988); Phys. Rep. **160**, 235 (1988).

[13]Rigorously we should also include the effect due to shadowing of the gluon structure function of the nucleus. A more detailed analysis may be able to distinguish quark and gluon shadowing effects.

[14]B. L. Ioffe, Phys. Lett. **30B**, 123 (1969); A. Suri and D. R. Yennie, Ann. Phys. (N.Y.) **72**, 243 (1972).

[15]V. Franco, Phys. Rev. Lett. **24**, 1452 (1970); Phys. Rev. C **6**, 748 (1972).

[16]A. Y. Abul-Magd, Nucl. Phys. **B8**, 638 (1968).

[17]R. A. Rudin, Phys. Lett. **30B**, 357 (1969).

[18]The relationship between the invariant amplitude $T_{\bar{q}N}$ and the laboratory-frame amplitude $F_{\bar{q}N}$ is given by $F_{\bar{q}N}(k, v^2, \mathbf{q}) = (k/8\pi p_{c\,m}\sqrt{s})T_{\bar{q}N}(s, v^2, \mathbf{q})$, and the optical theorem reads as follows:

$$\sigma_{\text{tot}} = \frac{4\pi}{k} \text{Im} F_{\bar{q}N}(k, v^2, 0) = \frac{1}{2p_{\text{c.m.}}\sqrt{s}} \text{Im} T_{\bar{q}N}(k, v^2, 0),$$

where k is the virtual quark's three-momentum in the laboratory frame, and $p_{\text{c.m.}} = [v^2 + (s - M^2 - v^2)^2/4s]^{1/2}$ is the three-momentum in the quark-nucleon center-of-mass system and M is the nucleon mass.
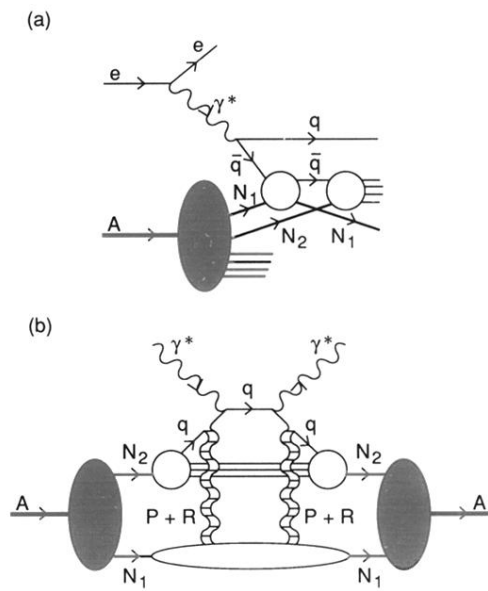
FIG. 1. (a) The double-scattering amplitude that shadows the direct interaction of the antiquark with N_2. (b) The same mechanism as in (a), drawn in the traditional "hand-bag" form. The Pomeron and Reggeon exchanges between the quark line and N_1 are explicitly illustrated.